Analysis of rate-of-rise of VFTO according to Switching Conditions in GIS

Hun-Chul Seo, Won-Hyeok Jang, Chul-Hwan Kim, Toshihisa Funabashi, Tomonobu Senju

Abstract--**Very Fast Transients (VFT) originate mainly from disconnetor or circuit breaker switching operations in Gas Insulated Substations (GIS). This paper conducts simulations using EMTP-RV in order to determine the rate-of-rise of Very Fast Transient Overvoltage (VFTO) according to the switching conditions in GIS. Each component of the GIS is modeled by distributed line models and lumped models based on equivalent circuits. The various disconnector switching or circuit breaker switching conditions are simulated, and the results are analyzed.**

Keywords: **Circuit breaker, Disconnector, EMTP-RV, Rate-of-Rise, Very Fast Transient Overvoltage**

I. INTRODUCTION

In GIS, VFTOs are generated during the switching operation of a Disconnect Switch (DS) or a Circuit Breaker (CB). During the switching operation, a number of pre-strikes or re-strikes occur because of the slow speed of the moving contact of DS. These strikes generate VFTO with very high frequency oscillations [1-8]. Even though their magnitudes are lower than Basic Insulation Level (BIL) of the system, they contribute to the aging on the insulation of the system due to their frequent occurrences. Also, VFTO can influence on the insulation of other GIS equipment such as transformers [9-11]. Hence, it is necessary to estimate the magnitudes and rate-of-rise of VFTO generated during switching operations for insulation coordination of GIS components.

This paper analyzes the rate-of-rise of VFTO at transformer terminals in a 550kV GIS using EMTP-RV. Firstly, the calculation methods of rate-of-rise are discussed. Secondly, the modeling of each component of GIS is presented. Each component is modeled by distributed line models and lumped models based on the equivalent circuits recommended by IEEE. Thirdly, the simulations with various DS and CB switching conditions are performed. Finally, all the cases of the rate-of-rise of VFTO according to the simulation conditions are discussed.

H. C. Seo, W. H. Jang, C. H. Kim are with the School of Information and Communication Engineering, Sungkyunkwan University, Suwon-city, 440-746, Korea (e-mail: hunchul0119@hanmail.net, bihyn@hanmail.net, hmwkim@hanmail.net).
Toshihisa. Funabashi is with Meidensha Corporation, Tokyo 141-6029 Japan(e-mail: funabashi-t@mb.meidensha.co.jp).
Tomonobu Senjyu is with the Department of Electrical and Electronics Engineering, University of the Ryukyus,Nishihara 903-0213, Japan (e-mail: b985542@tec.u-ryukyu.ac.jp).

II. RATE-OF-RISE OF VFTO

The rate-of-rise of VFTO can be defined in a various ways. The waveform of VFTO shows extremely radical fluctuations even on a microsecond timescale because of the characteristics of traveling wave refracted and reflected in a very short distance at GIS. Consequently, if the rate-of-rise is defined as max(dv/dt), it is possible to have a very large value regardless of the characteristics of targeted waveforms or simulation conditions. In this paper, therefore, other methods to calculate the rate-of-rise of voltage are discussed. The rate-of-rise of VFTO is defined as the magnitude of voltage per microsecond, i.e. in kV/µs in these methods.

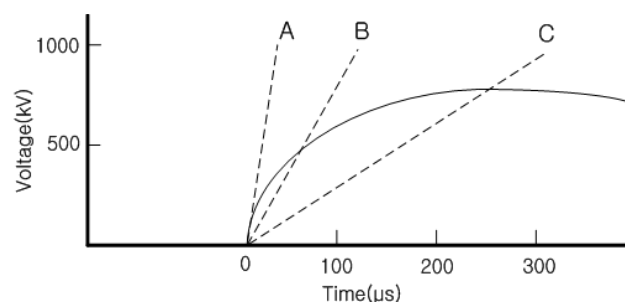Fig. 1 shows the methods to calculate the rate-of-rise of voltage [12].

Fig. 1. Methods to calculate rate-of-rise of voltage

In Fig. 1, the rate-of-rise can be calculated as follows:

1) A: the slope at t=0
2) B: the surge recorder measured rate-of-rise
3) C: the slope from t=0 to the first peak voltage

This paper calculates the rate-of-rise using method A among aforementioned three methods.

III. MODELING OF GIS USING EMTP-RV

A. GIS Model

The GIS in Fig. 2 consists of DS, circuit breakers, earthing switches, TR feeders, T/L feeders, busbars, coupling feeders, and etc. The rated voltage of GIS is 550kV. The number of generators connected to transformers is 46 and the capacity of each generator is 83.34MVA. In Fig. 2, L1~L5 indicate the T/L feeders and T1~T12 are the TR feeders. Also, circles signify the DS and rectangles express the circuit breakers. Fig. 2 shows the switching at steady state. The black circles and rectangles illustrate the close state and the white circles and rectangles indicate the open state.
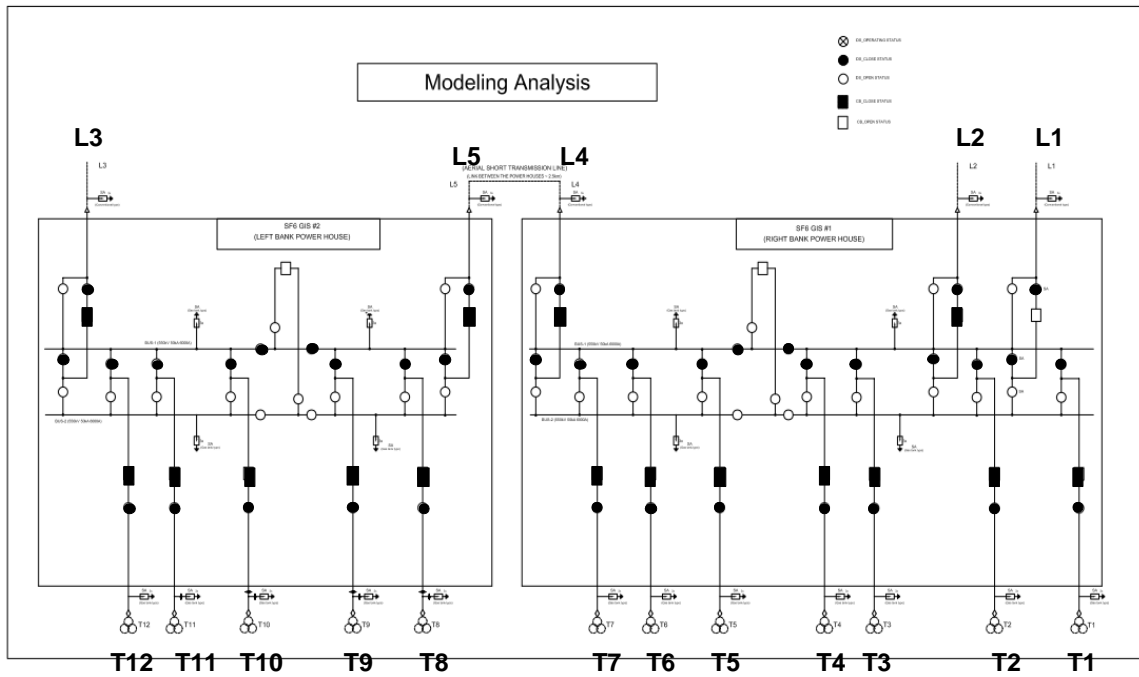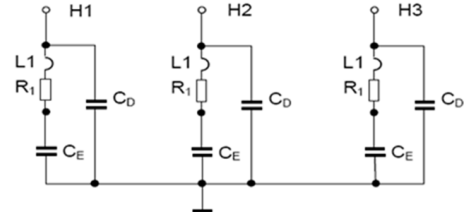
Fig. 2. GIS Model

B. Modeling of Each Component in GIS

Due to the travelling wave nature of VFTO in a GIS, modeling of the GIS components, such as a busbar, a circuit breaker, and a DS, makes use of electrical equivalent circuits composed of lumped elements and distributed parameter lines. Therefore, this paper performs the modeling of each component using the values recommended by IEEE as shown in Table I [1-4].

The parameters such as resistance, surge impedance, and propagation time, of transmission lines, used to model the busbar, the circuit breakers, and the DS, are calculated by EMTP-RV using the geometrical and electrical data of a cable of EMTP-RV to model the GIS [13-15]. In case of the circuit breaker, the capacitance of 430pF between each pole is added. These data are inputted to the distributed line model.

C. Modeling of Transformer

The modeling of a transformer can be performed by the VFT transformer model as shown in Fig. 3. In this model, low voltage terminals and neutral are grounded.

- L1 = HV bushing and connection inductance
- R1 = HV bushing ohmic resistance
- C_D = HV bushing capacitance to earth
- C_E = Winding capacitance

Fig. 3. VFT transformer model

TABLE I
EQUIVALENT MODELING OF GIS COMPONENTS

GIS component	Equivalent model		
Bus bar	Transmission line model (untransposed)		
Circuit Breaker	open state		close state	
Disconnect Switch	open state		close state	
Surge Arrester	Capacitance to ground: 50pF		
Earthing Switch	Capacitance to ground: 45pF		
Bushing	Capacitance to ground: 500pF		

A. Simulation Conditions

This paper conducts the simulation of VFTO occurred by closing a DS or a CB at each feeder in Fig. 2. Table II shows the simulation conditions. Case 1, 2, 3, 10, and 11 are the cases of closing a DS or a CB at the T/L feeder L1, L2, L3, L4 and L5, respectively. Case 4, 5, 6, 7, 8, and 9 are the cases of closing a DS or a CB at the TR feeder T1, T4, T7, T8, T10 and T12, respectively. For each case, the simulations according to the various closing point-on-wave are simulated.

TABLE II
SIMULATION CONDITIONS

Case		Feeder	Operating Equipment
Case 1	Case 1-1	L1	DS
	Case 1-2		CB
Case 2	Case 2-1	L2	DS
	Case 2-2		CB
Case 3	Case 3-1	L3	DS
	Case 3-2		CB
Case 4	Case 4-1	T1	DS
	Case 4-2		CB
Case 5	Case 5-1	T4	DS
	Case 5-2		CB
Case 6	Case 6-1	T7	DS
	Case 6-2		CB
Case 7	Case 7-1	T8	DS
	Case 7-2		CB
Case 8	Case 8-1	T10	DS
	Case 8-2		CB
Case 9	Case 9-1	T12	DS
	Case 9-2		CB
Case 10	Case 10-1	L4	DS
	Case 10-2		CB
Case 11	Case 11-1	L5	DS
	Case 11-2		CB

B. Simulation Results

In this paper, the simulation results for Case 1 are presented. Fig. 4 shows the GIS model for Case 1-1 which is the case of closing a DS at the T/L feeder L1. Fig. 5 shows the waveform of the VFTO simulated at the transformer T1 when the closing point-on-wave for Case 1-1 is 90°. The VFTO waveform represents the characteristics of a travelling wave and the maximum magnitude of the VFTO is 1.515pu.

Fig. 6 shows the GIS model for Case 1-2 which is the case of closing a CB at the T/L feeder L1. Fig. 7 represents the waveform of the VFTO simulated at the transformer T1 when the closing point-on-wave for Case 1-2 is 90°. The maximum magnitude of the VFTO is 1.732pu. We can find that the maximum magnitude of the VFTO for Case 1-2 is larger than one for Case 1-1.
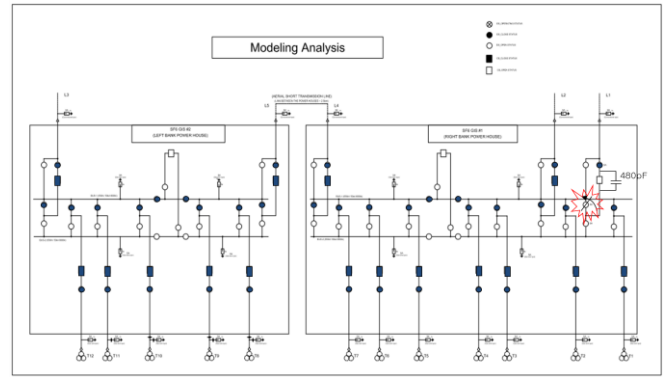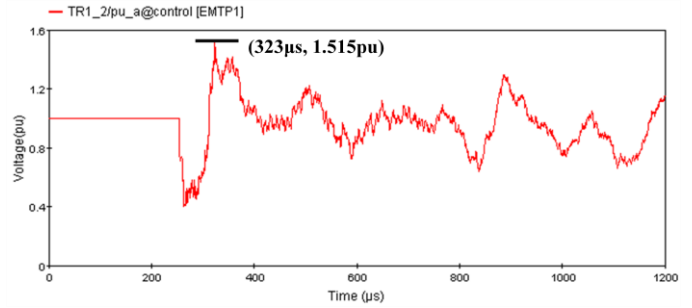

Fig. 4. GIS model for Case 1-1

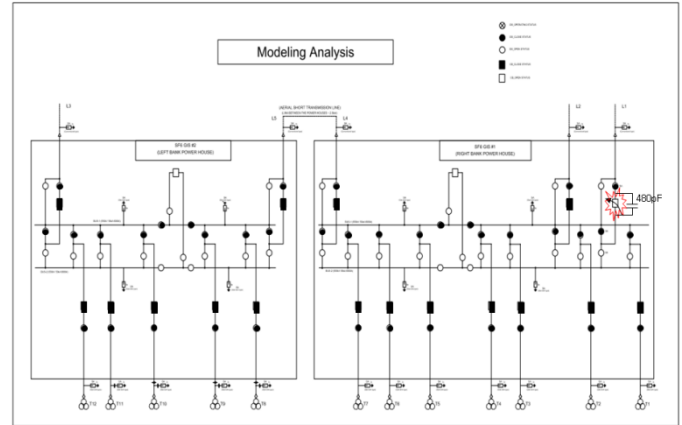Fig. 5. Waveform of the VFTO simulated at the transformer T1 when the closing point-on-wave Case 1-1 is 90°
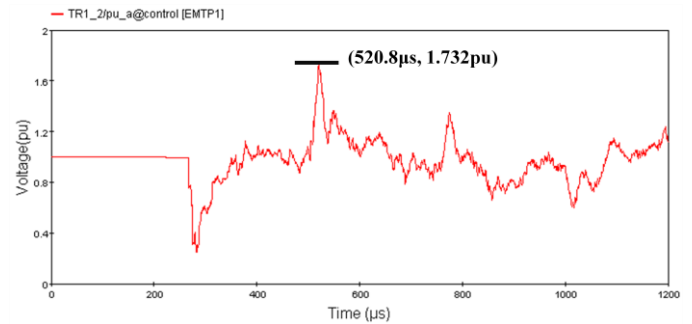

Fig. 6. GIS model for Case 1-2

Fig. 7. Waveform of the VFTO simulated at the transformer T1 when the closing point-on-wave for case 1-2 is 90°

C. Discussion

In each of Case 1, 2, 3, 10, and 11, the measuring point of the maximum magnitude and rate-of-rise of VFTOs is the same

for both cases of closing a DS and closing a CB at each T/L feeder. In each of Case 4, 5, 6, 7, 8 and 9, however, the measuring point of the maximum magnitude and rate-of-rise of VFTO in cases of closing a DS is different from one in cases of closing a CB at each TR feeder. The reason for this phenomenon can be explained with the surge propagation routes as shown in Fig. 8 and Fig. 9. The circled numbers on surge propagation route in Fig. 8 and Fig. 9 represent the sequence of the surge propagation after operating DS or operating CB is closed. When operating DS is closed, the surge from operating DS is propagated toward measuring point 1 and 2 as shown in Fig. 8. However, the CB on route toward measuring point 2 is open so that the surge cannot be reached to measuring point 2 and the maximum magnitude and rate-of-rise of VFTO is occurred at measuring point 1. In Fig. 9, when operating CB is closed, the surge from operating CB is propagated toward both sides. Unlike the circuit in Fig. 8, the surge can be reached to both measuring point 1 and measuring point 2 since operating DS is supposed to be closed before operating CB is closed.
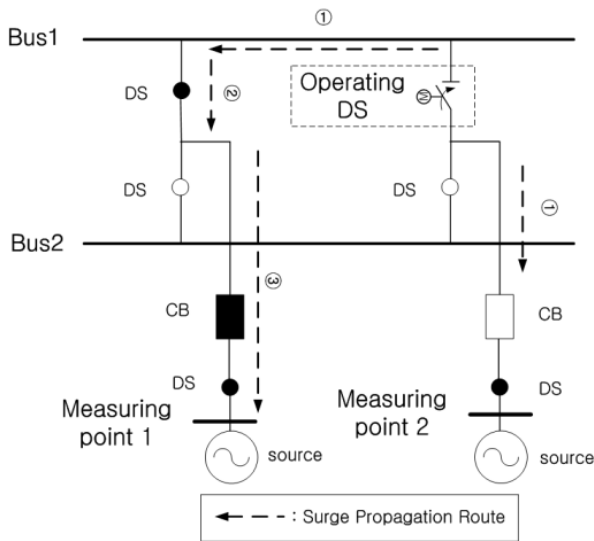

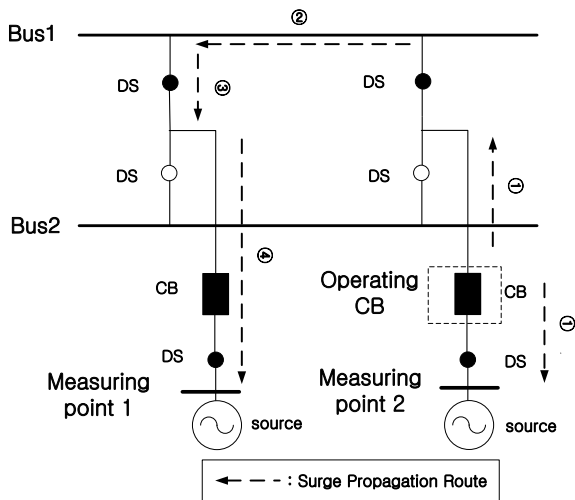Fig. 8. Simplified equivalent circuit for cases of closing a DS at a TR feeder

Fig. 9. Simplified equivalent circuit for cases of closing a CB at TR feeder

In the paper, there are four points to analyze. The first is magnitudes of VFTO when closing a DS or a CB. The second is rates-or-rise of VFTO in the cases of closing a DS or a CB with 90° of closing point-on-wave where maximum values can be found. The third is rates-of-rise of VFTO according to various closing points-on-wave for the cases of closing a DS or a CB. The last is rate-of-rise of VFTO for each case when the closing point-on-wave is equal.

First, we compare the magnitudes of VFTO in the cases of closing a DS and the ones in the cases of closing a CB. Fig. 10 shows the comparison of the maximum magnitudes of VFTO in the cases of closing a DS and a CB at each T/L feeder. The biggest among the maximum magnitudes of VFTO in the cases of closing a CB is 1.94pu and the one in the cases of closing a DS is 1.515pu. For all the cases in Fig. 10, the maximum magnitude of VFTO when closing a CB is always larger than the one when closing a DS. Fig. 11 compares the magnitudes of VFTO in the cases of closing a DS and the one in the cases of closing a CB at each TR feeder. In the cases of closing a CB, the maximum magnitudes of VFTO simulated at measuring point 2 are approximately 1.75pu while the magnitudes simulated at measuring point 1 vary from 1.2pu to 1.45pu. In the cases of closing a DS, the maximum magnitudes of VFTO are around 1.25pu. For all the cases, the magnitudes at measuring point 2 when closing a CB are much larger than the magnitudes at measuring point 1 when closing a DS and the difference is approximately 0.5pu. Also, the magnitudes of VFTO simulated at measuring point 1 for cases of closing a CB are larger than one for cases of closing a DS except Case 7.
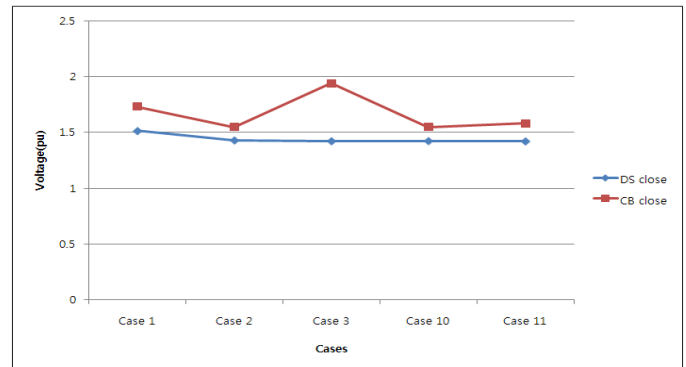

Fig. 10. Comparison of the maximum magnitudes of VFTO in the cases of closing a DS and a CB at T/L feeder
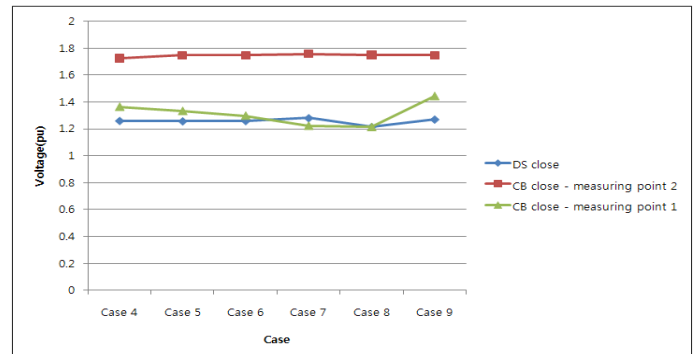

Fig. 11. Comparison of the maximum magnitudes of VFTO in the cases of closing a DS and a CB at TR feeder

Secondly, we compare the rate-of-rise of VFTO for the cases of closing a DS and for the cases of closing a CB, with 90° of closing point-on-wave where maximum values can be found. Fig. 12 compares the rate-of-rise of VFTO in the cases of closing a DS and a CB at T/L feeders. The rate-of-rise of VFTO when closing a DS is larger than the one when closing a CB in each Case and the differences are approximately 95kV/μs as shown in Fig. 12. Fig. 13 compares the rate-of-rise of VFTO with a DS closed and the one with a CB closed at TR feeders. For all the cases of closing a CB, the rate-of-rise simulated at measuring point 2 is unchanged at 3045 kV/μs. This is because of the same cable parameters of TR feeders. This value is the maximum rate-of-rise simulated in the whole simulations and is approximately 2700 kV/μs larger than the rate-of-rise at measuring point 1 in the cases of closing a DS. At measuring point 1, the rate-of-rise when closing a DS is always larger than the one when closing a CB for all the cases as shown in Fig. 13 and the difference varies from 45 to 90kV/ μs case by case.
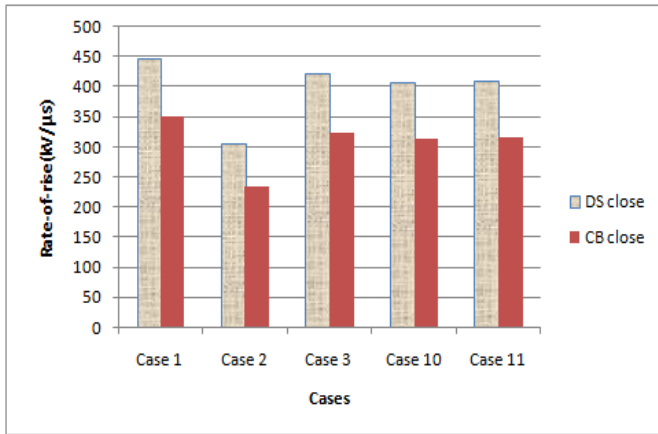

Fig. 12. Comparison of the rate-of-rise of VFTO in the cases of closing a DS and a CB at T/L feeder
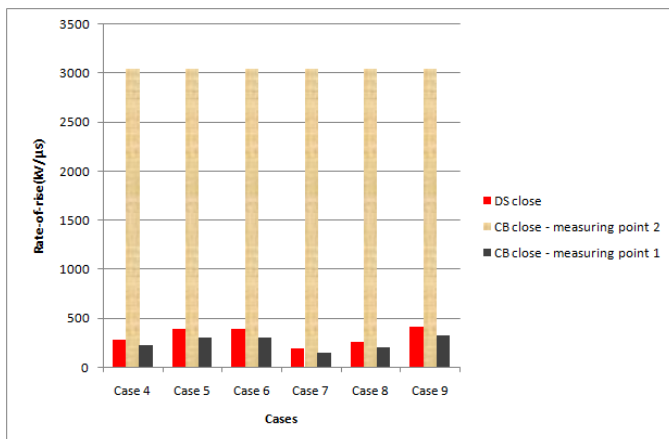

Fig. 13. Comparison of the rate-of-rise of VFTO in the cases of closing a DS and a CB at TR feeder

Although all the simulation conditions are same, the rate-of-rise value is not same at measuring point 1 and at measuring point 2. This phenomenon is due to the difference of surge propagation route described in Fig. 8 and Fig. 9. When operating CB at the TR feeder is closed, measuring point 2 is

closer from operating CB than measuring point 1 as shown in Fig. 9 and therefore the surge from operating CB to measuring point 2 has a shorter surge propagation route than to measuring point 1. Even if the measuring point is the same, the propagation route can still be different according to which equipment is closed. When comparing rates-of-rise simulated at measuring point 1, the case of closing a DS has shorter surge propagation route than the case of closing a CB as shown in Fig. 8 and Fig. 9. A shorter surge propagation route means shorter propagation time provided that the resistance is proportional to the length of the route. Therefore, shorter propagation time indicates that the route has smaller resistance and vice versa. As the resistance on the route is smaller, the damping of surge also becomes smaller, and consequently, the rate-of-rise becomes higher.

Thirdly, we compare the rate-of-rise of VFTO according to the closing point-on-wave for the cases of closing a DS and the cases of closing a CB. Fig. 14 shows the rate-of-rise of VFTO according to the various closing points-on-wave for the cases of closing a DS. As the closing point-on-wave approaches 90° and 270°, the rate-of-rise increases as shown in Fig. 14. On the other hand, as the closing point-on-wave approaches 0° and 180°, the rate-of-rise decreases. Also, the increasing rate and the decreasing rate have approximate linearity.
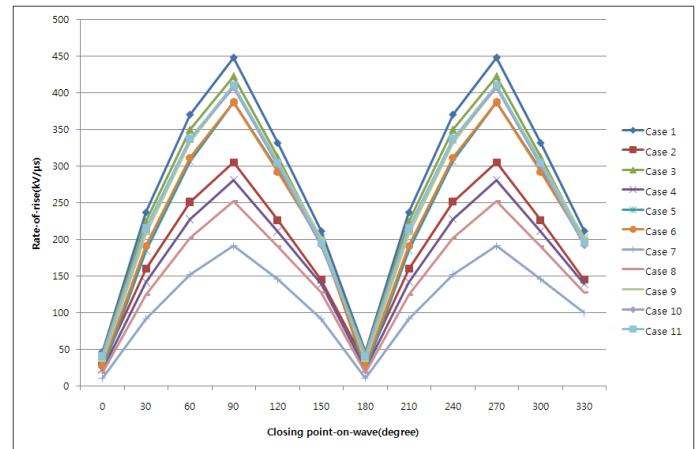

Fig. 14. Rate-of-rise of VFTO according to various closing points-on-wave for cases of closing a DS

Fig. 15 shows the rate-of-rise of VFTO according to the various closing points-on-wave for the cases of closing a CB at each T/L feeder. Rates-of-rise in Fig. 15 have a very similar pattern as Fig. 14. Fig. 16 and Fig. 17 show the rate-of-rise of VFTO simulated at measuring point 2 and measuring point 1, respectively, according to various closing points-on-wave for the cases of closing a CB at TR feeders. The graphs also have a similar pattern as Fig. 14 and Fig. 15. However, the difference is that Fig. 14 and Fig. 15 have linearity regardless of closing point-on-wave while Fig. 16 and Fig. 17 have linearity except 60°~120° and 240°~300° of closing points-on-wave. Also, as shown in Fig. 16, the rates-of-rise of VFTO simulated at measuring point 2 at each closing point-on-wave have the same value for all the cases. This is because the cable parameters on TR feeder are the same for all the cases.
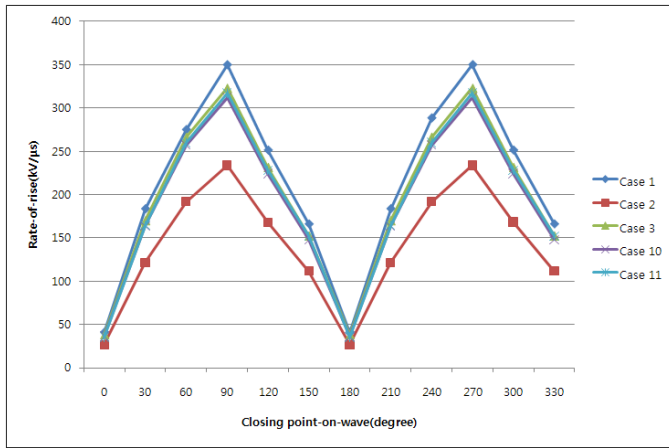
Fig. 15. Rate-of-rise of VFTO according to various closing points-on-wave for cases of closing a CB at T/L feeders
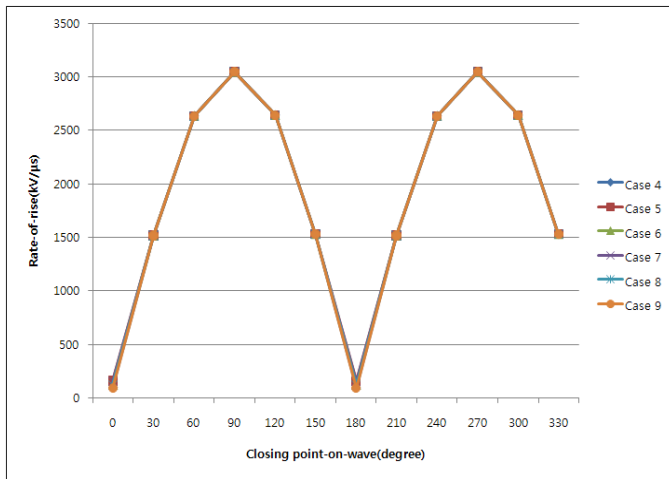

Fig. 16. Rate-of-rise of VFTO simulated at measuring point 2 according to various closing points-on-wave for cases of closing a CB at TR feeders
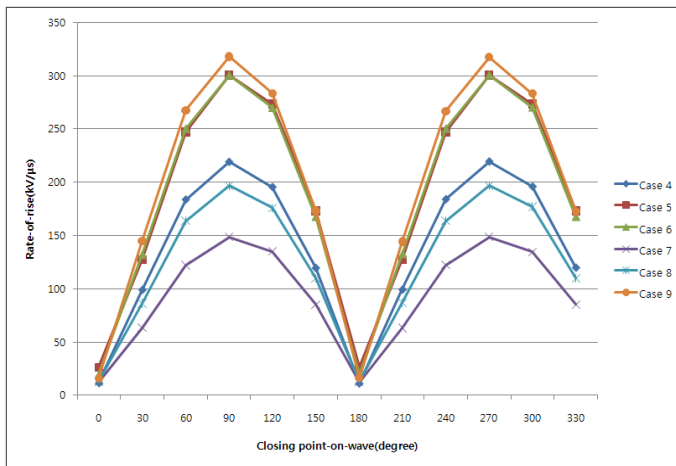

Fig. 17. Rate-of-rise of VFTO simulated at measuring point 1 according to various closing points-on-wave for cases of closing a CB at TR feeders

Finally, we compare the rate-of-rise of VFTO for each case when the closing point-on-wave is equal. Even though simulations are conducted at the same closing points-on-wave in each case, the rates-of-rise of the VFTO are all different from each case as shown in Fig. 14, Fig. 15, and Fig. 17. The reason for this can be explained by two factors; the number of branches on the surge propagation route and the surge

propagation time from DS to transformer terminals as shown in Table III. In Table III, cases are organized in descending order of rate-of-rise. In general, the cases with T/L operating feeders have shorter surge propagation time from the DS to the transformer terminal than the cases with TR operating feeders. This is because the surge propagation distance is shorter in T/L feeders than in TR feeders. Comparing cases with similar surge propagation times, but different number of branches on the surge propagation route, Case 1, 3, 10 and 11 have higher rate-of-rise than Case 2 as well as Case 5, 6 and 9 have higher rate-of-rise than Case 4 and 7. From this result, we can conclude that as the number of branches on the route increases, the rate-of-rise decreases.

TABLE III
COMPARISON OF SIMULATION RESULTS IN DESCENDING ORDER
OF RATE-OF-RISE

Case	Rate-of-rise (kV/μs)	Operating feeder	Branches on surge propagation route and resistance	Surge propagation time from DS to transformer terminal (μs)
1	448.314	T/L		255
3	422.870			226
11	410.628	T/L		240
10	407.790			240
9	409.691			301
6	387.520	TR		363
5	387.057			363
2	305.300	T/L		240
4	281.102	TR		363
8	252.255	TR		363
7	191.542			363

V. CONCLUSIONS

In this paper, analysis of the rate-of-rise of VFTO is conducted using EMTP-RV. For GIS components, such as DS, circuit breakers, busbars, and etc., the modeling based on electrical equivalent circuits is performed. Also, in the case of transformers, the VFT model given by the manufacturer is used. The various switching conditions are simulated and the analysis results can be summarized as follows;

1) In the cases of closing a CB at T/L feeders, the maximum magnitudes of VFTO simulated at measuring point 2 are approximately 1.75pu while the magnitudes simulated at measuring point 1 vary from 1.2pu to 1.45pu. In the cases of closing a DS at T/L feeders, the maximum magnitudes of VFTO are around 1.25pu.

2) The magnitude of VFTO simulated at measuring point 1 and 2 when closing a CB is always larger than one when closing a DS except Case 7.

3) The rate-of-rise of VFTO when closing a DS is larger than the one when closing at TR feeders, and the differences are approximately 95kV/μs

4) When closing a CB at TR feeders, the rates-of-rise simulated at measuring point 2 are the same regardless of closing points-on-wave.

5) For all the cases of closing a CB, the rate-of-rise simulated at measuring point 2 is unchanged at 3045 kV/μs due to the same cable parameters of TR feeders. This is approximately 2700 kV/μs larger than the rate-of-rise at measuring point 1 in the cases of closing a DS.

6) As the surge propagation time from the DS or CB to the measuring point is shorter, the rate-of-rise is increased and vice versa.

7) Regardless of switched DS or CB, as the closing point-on-wave approaches the maximum value of the surge voltage, i.e. 90° and 270°, the rate-of-rise increases, while as the closing point-on-wave approaches the minimum value of voltage, i.e. 0° and 180°, the rate-of-rise decreases.

8) As the surge propagation time from the DS or CB to the transformer terminal is shorter, the rate-of-rise is increased and vice versa.

9) As the number of branches on the surge propagation route is increased, the rate-of-rise is decreased and vice versa.

VI. REFERENCES

[1]   IEEE PES Special Publication, "Tutorial on Modeling and Analysis of System Transients using Digital Programs", IEEE Working Group 15.08.09, 1998.

[2]   D. Povh, H. Schmeitt, O. Volcker, and R. Witzmann, "Modeling and Analysis Guidelines for Very Fast Transients", *IEEE Trans. on Power Delivery*, Vol. 11, No. 4, pp. 2028-2035, October, 1996.

[3]   J. Meppelink, K. Diederich, K. Feser, W. Pfaff, "Very Fast Transients in GIS", *IEEE Trans. on Power Delivery*, Vol. 4, No. 1, pp. 223-233, January, 1989.

[4]   V. Vinod Kumar, Joy Thomas M., M.S. Naidu, "Influence of Switching Conditions on the VFTO Magnitudes in a GIS", *IEEE Trans. on Power Delivery*, Vol. 16, No. 4, pp. 539-544, Oct., 2001.

[5]   A. Tavakoli, A. Gholami, A. Parizad, H. M. Soheilipour, H. Nouri, "*Effective Factors on the Very Fast Transient Currents and Voltages in the GIS*", IEEE Transmission & Distribution Conference & Exposition: Asia and Pacific, 2009.

[6]   Q. Liu, "Study of Protection of Transformer from Very Fast Transient Over-voltage in 750kV GIS", International Conference on Electrical Machines and Systems, Vol. 3, pp. 2153-2156, 2005.

[7]   Tian Chi, Lin Xin, Xu Jianyuan, Geng Zhen-xin, "Comparison and Analysis on Very Fast Transient Overvoltage Based on 550kV GIS and 800kV GIS", International Conference on High Voltage Engineering and Application, Chongqing, China, November 9-13, 2008

[8]   Qing Liu, Yufeng Zhang, "Influence of Switching Conditions on Very Fast Transient Over-voltage in 500kV Gas Insulated Substation", International Conference on Electrical Machines and Systems, 2008.

[9]   J. Amamathl, D.R.K. Paramahamsa, K. Narasimharao, B.P.Singh, K.D. Shrivastava, "Very fast transient over-voltages and transient enclosure voltages in gas insulted Substations", 2003 Annual Report Conference on Electrical Insulation and Dielectric Phenomena.

[10] Allan Greenwood, "Electrical Transients in Power Systems", John Wiley & Sons 1991.

[11] Van der Sluis, "Transients in Power System", John Wiley & Sons 2001.

[12] Dean E. Perry, Richard C. Raupach, C. A. EDWARD, "A Switching Surge Transient Recording Device", *IEEE Trans. on Power Apparatus and Systems*, Vol. PAS-87, No. 4, pp. 1073-1078, April, 1968.

[13] DCG-EMTP(Development coordination group of EMTP) Version EMTP-RV, Electromagnetic Transients Program. [Online]. Avaliable : http://www.emtp.com.

[14] Keon-Woo Park, Hun-Chul Seo, Chul-Hwan Kim, Chang-Soo Jung, Yeon-Pyo Yoo, Yong-Hoon Lim, "Analysis of the Neutral Current for Two-Step-Type Poles in Distribution Lines", *IEEE Transactions on Power Delivery*, Vol. 24, No. 3, pp. 1483-1489, July 2009.

[15] Hun-Chul Seo, Chul-Hwan Kim, Sang-Bong Rhee, Jae-Chul Kim, Ok-Bae Hyun, "Superconducting Fault Current Limiter Application for Reduction of the Transformer Inrush Current: A Decision Scheme of the Optimal Insertion Resistance", *IEEE Trans. on Applied Superconductivity*, Vol. 20, No. 4, pp. 2255-2264, August 2010.